IJBEM
Vol. 7, No. 2, 2005

Detection of cortical patch activity in beamspace using the generalized likelihood ratio test

T. Limpiti[1], A. K. Bolstad[1], B. D. Van Veen[1], and R. T. Wakai[2]
[1]Department of Electrical and Computer Engineering, University of Wisconsin-Madison, WI, USA
[2]Department of Medical Physics, University of Wisconsin-Madison, WI, USA

***Abstract*— A multi-stage algorithm for detecting and imaging distributed neural activity is presented. The signal of interest is assumed to originate from an unknown patch of cortex. The signal is modeled as the mean component of noisy measurements, where the noise is assumed to be Gaussian with unknown spatial covariance R_s and known temporal covariance R_t. We define patches on the cortical surface and perform a detection step using the generalized likelihood ratio test to identify the patch with the most significant activity. This patch identification step is performed in beamspace to reduce the data dimension and increase the effective signal-to-noise ratio. Next, the unknown signal originating from the patch is estimated using the maximum likelihood criterion. Finally, we reconstruct an image of activity within the patch by solving a local inverse problem using the estimated patch signal. We demonstrate the effectiveness of our method using both real and simulated evoked response data.**

***Keywords*— MEG inverse problem, multi-stage source imaging, beamspace, cortical bases, maximum likelihood.**

I. Introduction

Detection and imaging of distributed neural activity from electro- and magnetoencephalographic (EEG/MEG) data is extremely challenging due to the severe ill-posedness of the inverse problem and relatively low signal to noise ratio (SNR) common in EEG/MEG. The often used equivalent current dipole (ECD) model is inadequate for representing distributed activity because the extent of the source cannot be determined. On the other hand, nonparametric distributed source models lead to underdetermined, nonunique solutions to the inverse problem. Cortical patch [1], [2] and multipole [3], [4], [5] source models have been proposed to overcome these limitations.

We present a multi-stage approach for source detection and imaging using cortical patch models, in which the best patch is identified using the generalized likelihood ratio test (GLRT), the signal originating from the patch is estimated using the maximum likelihood (ML) criterion, and the activity within the patch is imaged by solving a local inverse problem. The ML criterion has been applied to EEG/MEG source localization and signal estimation in [6], [7]. Our application is distinguished by the cortical patch signal model. Multi-stage detection and imaging methods have also been proposed using dipolar [8], [9] and multipolar [5] source models. Both [8] and [9] involve a coarse to fine search strategy, while [5] involves first estimating the multipole parameters and then using the estimates to identify a source distribution.

A key aspect of our approach is the use of spatial basis function expansions for representing the signal originating from each cortical patch. Fewer spatial bases are employed for patch localization than signal estimation in order to increase the differentiation between candidate patches. Localization is performed after transforming the data into beamspace [10], [11], which reduces data requirements and improves localization performance [10]. The patch that has the largest GLRT statistic is declared to contain the source of activity and the ML estimate of the signal from this patch is calculated. A relatively large number of spatial basis functions is employed for signal estimation. In this paper, the distribution of cortical activity within the patch is estimated using a minimum norm solution to the local inverse problem. Simulated and real somatosensory evoked response data are presented to demonstrate the method.

Bold uppercase and lowercase symbols represent matrix and vector quantities, respectively. Superscript T and -1 are used to denote matrix transpose and matrix inverse.

II. Methods

A. Data model

We assume the signal component of the data is repeatable across epochs and randomness from epoch to epoch is due to noise. Given J epochs of spatiotemporal measurements from N sensors and T samples in time, we represent the j^{th} $N \times T$ data matrix $\mathbf{X}_j$ as

$$\mathbf{X}_j = \mathbf{U}\mathbf{A}\mathbf{C}^T + \mathbf{N}_j, \quad j = 1, \ldots, J. \tag{1}$$

where the mean, or signal, $\mathbf{S} = \mathbf{U}\mathbf{A}\mathbf{C}^T$, is expressed in terms of a known $N \times P$ spatial basis matrix $\mathbf{U}$, a known $T \times L$ temporal basis matrix $\mathbf{C}$, and an unknown $P \times L$ signal amplitude matrix $\mathbf{A}$. $\mathbf{N}_j$ is the noise component, assumed to be zero-mean Gaussian with unknown spatial covariance $\mathbf{R}_s$ and known temporal covariance $\mathbf{R}_t$. The noise is assumed independent across epochs. Without loss of generality $\mathbf{R}_t = \mathbf{I}$ is used in the sequel.

The columns or spatial distribution of the signal matrix $\mathbf{S}$ lies in the space spanned by the columns of $\mathbf{U}$, while the rows or time evolution lies in the space spanned by the columns of $\mathbf{C}$. The temporal basis matrix $\mathbf{C}$ is constructed to represent signals from the frequency band of interest, as suggested in [7]. Each cortical patch is represented by a different set of spatial bases $\mathbf{U}$ and amplitude parameters $\mathbf{A}$. Construction of

$\mathbf{U}$ is described in subsection II-C while estimation of $\mathbf{A}$ is described in subsection II-E.

Concatenating all data epochs together, we form a new $N \times JT$ data matrix

$$\begin{aligned}\mathbf{X} &= [\mathbf{X}_1\, \mathbf{X}_2\, \ldots\, \mathbf{X}_J] \\ &= \mathbf{U}\mathbf{A}\mathbf{D}^T + \mathbf{N} \end{aligned} \quad (2)$$

where $\mathbf{D}^T = \left[\mathbf{C}^T\, \mathbf{C}^T\, \ldots\, \mathbf{C}^T\right]$ and $\mathbf{N} = [\mathbf{N}_1\, \mathbf{N}_2\, \ldots\, \mathbf{N}_J]$. We write the Gaussian probability density for $\mathbf{X}$ as $\mathbf{X} \sim \mathcal{N}\left(\mathbf{U}\mathbf{A}\mathbf{D}^T, \mathbf{R}_s \otimes \mathbf{I}\right)$ [12].

B. Beamspace transformation

Beamspace processing involves projecting the data into a smaller dimensional space with minimal loss of signal [13], [14]. It is particularly useful for applications with limited data samples and algorithms that involve estimating a spatial covariance matrix from the data. It has been shown to produce more stable localization results than sensor space processing [10]. We construct the beamspace transformation $\mathbf{F}$ to approximately span the space defined by all lead field matrices in the anatomical region of interest, which may be as large as the entire cortex. Following [10], the criterion for choosing $\mathbf{F}$ is minimization of the mean squared representation error (MSRE) between the sensor space and the beamspace lead field matrices. That is, if $\mathbf{H}(\theta_i)$ is the lead field matrix for a dipolar source located at θ_i within a region of interest, then

$$\begin{aligned}\mathbf{F} &= \arg\min_{\mathbf{F}} \sum_{i=1}^{q} \mathbf{H}(\theta_i)^T \left(\mathbf{I} - \mathbf{F}\mathbf{F}^T\right) \mathbf{H}(\theta_i) && (3)\\ &= \arg\max_{\mathbf{F}}\ \mathrm{tr}\left\{\mathbf{F}^T\mathbf{G}\mathbf{F}\right\} && (4)\end{aligned}$$

where $\mathbf{G} = \sum_{i=1}^{q} \mathbf{H}(\theta_i)\mathbf{H}(\theta_i)^T$ and $\mathbf{F}$ is subject to the constraint $\mathbf{F}^T\mathbf{F} = \mathbf{I}$. The solution to (4) is to choose $\mathbf{F}$ as the eigenvectors of $\mathbf{G}$ corresponding to the M largest eigenvalues. The MSRE is controlled by the choice of M. The $M \times JT$ beamspace data $\mathbf{Z}$ is obtained by applying the beamspace transformation to the measurement data, $\mathbf{Z} = \mathbf{F}^T\mathbf{X}$. Then, $\mathbf{Z} \sim \mathcal{N}\left(\mathbf{F}^T\mathbf{U}\mathbf{A}\mathbf{D}^T, \mathbf{R}_b \otimes \mathbf{I}\right)$, where $\mathbf{R}_b = \mathbf{F}^T\mathbf{R}_s\mathbf{F}$ is $M \times M$.

C. Patch Construction

We define K overlapping cortical patches to completely cover the cortical surface of interest. Denote the candidate patches as $P_k,\ k = 1, \ldots,\ K$. The beamspace signal contributed by patch P_k is

$$\mathbf{F}^T\mathbf{S}_k = \mathbf{U}_k\mathbf{A}_k\mathbf{D}^T,\ k = 1,\ \ldots\ , K. \quad (5)$$

Here $\mathbf{U}_k$ is constructed by finding a basis for the space spanned by the beamspace lead field matrices of all dipoles in the patch. Specifically, we identify $\mathbf{U}_k$ by selecting the left singular vectors of a matrix $\mathbf{T}_k$ formed by concatenating the beamspace lead field matrices of all dipoles in P_k. That is, if $\theta_i^k,\ i = 1, 2, \ldots, q_k$, denotes the dipole locations in P_k, we have

$$\begin{aligned}\mathbf{T}_k &= \left[\mathbf{F}^T\mathbf{H}(\theta_1^k)\ \mathbf{F}^T\mathbf{H}(\theta_2^k)\ \ldots\ \mathbf{F}^T\mathbf{H}(\theta_{q_k}^k)\right] \\ &\approx \mathbf{U}_k\mathbf{\Sigma}_k\mathbf{V}_k^T && (6)\end{aligned}$$

where $\mathbf{U}_k$ and $\mathbf{V}_k$ are matrices of the left and right singular vectors of $\mathbf{T}_k$ and $\mathbf{\Sigma}_k$ contains the corresponding singular values. The singular value decomposition is necessary because $\mathbf{T}_k$ is usually rank deficient. The number of singular vectors selected for $\mathbf{U}_k$ differs for patch localization and patch signal estimation. A relatively small number is chosen for patch localization so that the $\mathbf{U}_k$ for distinct patches are better differentiated. Once the significant patch is identified, the number is increased to better estimate the signal originating from that patch.

D. Patch Localization

Patch localization is accomplished by choosing the patch associated with the maximum value of the GLRT statistics for testing $\mathbf{A}_k = 0$ vs. $\mathbf{A}_k \neq 0$. The GLRT statistic is formed by substituting maximum likelihood estimates of the unknown parameters $(\mathbf{A}_k, \mathbf{R}_b)$ into the likelihood ratio. Our derivation follows [7] and [15]. We first introduce

$$\begin{aligned}\mathbf{Z}_D &= \mathbf{Z}\mathbf{D}\left(\mathbf{D}^T\mathbf{D}\right)^{-1/2} && (7)\\ \mathbf{Z}_{\bar{D}} &= \mathbf{Z}\bar{\mathbf{D}} && (8)\\ \mathbf{Q}_{\bar{D}} &= \mathbf{Z}_{\bar{D}}{\mathbf{Z}_{\bar{D}}}^T && (9)\end{aligned}$$

with $\mathbf{D}^T\bar{\mathbf{D}} = \mathbf{0}$. The transformations $\mathbf{D}\left(\mathbf{D}^T\mathbf{D}\right)^{-1/2}$ and $\bar{\mathbf{D}}$ project the beamspace data $\mathbf{Z}$ onto two orthogonal subspaces. Since the signal time evolution lies in the space spanned by the rows of $\mathbf{D}$ and $\mathbf{D}^T\bar{\mathbf{D}} = \mathbf{0}$, $\mathbf{Z}_D$ contains the signal whereas $\mathbf{Z}_{\bar{D}}$ is signal-free. $\mathbf{Q}_{\bar{D}}$ can be viewed as a noise sample covariance matrix estimate.

The GLRT statistic for patch P_k can be shown to have the form [15],

$$l_k = \frac{\left|\mathbf{U}_k^T\mathbf{Q}_{\bar{D}}^{-1}\mathbf{U}_k\right|}{\left|\mathbf{U}_k^T\left(\mathbf{Z}\mathbf{Z}^T\right)^{-1}\mathbf{U}_k\right|} \quad (10)$$

The patch which has the largest GLRT statistic is selected as the one containing the source. In selecting only one patch, we are implicitly assuming that the spatial extent of the source is contained within the support of a single patch.

E. Patch Signal Estimation

Suppose that patch P_0 is identified as the significant patch. The signal originating from this patch is estimated by determining the amplitude parameters $\mathbf{A}_0$. In this stage we increase the number of left singular vectors used as bases in $\mathbf{U}_0$ to minimize the signal representation error. The maximum likelihood estimate of $\mathbf{A}_0$ is the solution to the minimization problem

$$\min_{\mathbf{A}_0} \left|\left(\mathbf{Z} - \mathbf{U}_0\mathbf{A}_0\mathbf{D}^T\right)\left(\mathbf{Z} - \mathbf{U}_0\mathbf{A}_0\mathbf{D}^T\right)^T\right| \quad (11)$$

which is given by [7], [15]

$$\hat{\mathbf{A}}_0 = \left(\mathbf{U}_0^T\mathbf{Q}_{\bar{D}}^{-1}\mathbf{U}_0\right)^{-1}\mathbf{U}_0^T\mathbf{Q}_{\bar{D}}^{-1}\mathbf{Z}_D\left(\mathbf{D}^T\mathbf{D}\right)^{-1/2} \quad (12)$$

The beamspace signal from P_0 is thus estimated as $\mathbf{U}_0\hat{\mathbf{A}}_0\mathbf{C}^T$.

F. Local inverse solution

In the last stage the estimated signal is used to reconstruct an image of neural activity within the patch P_0. The local inverse problem on P_0 is generally much better conditioned than the original global inverse problem. Many methods can be used to solve the local inverse problem. Here we choose the minimum norm method for illustration. Let $\mathbf{M}_0$ be a matrix whose rows contain the dipole moment time series corresponding to the columns of $\mathbf{T}_0$ defined in (6). The local inverse problem for $\mathbf{M}_0$ is expressed as $\mathbf{T}_0\mathbf{M}_0 = \mathbf{U}_0\hat{\mathbf{A}}_0\mathbf{C}^T$. The minimum norm solution for $\mathbf{M}_0$ is given by

$$\hat{\mathbf{M}}_0 = \left(\mathbf{T}_0^T\mathbf{T}_0\right)^- \mathbf{T}_0^T\mathbf{U}_0\hat{\mathbf{A}}_0\mathbf{C}^T$$

where $(\,\cdot\,)^-$ denotes the pseudo inverse operation.

III. Results

Simulated data is obtained by generating 300 epochs of evoked response data for each SNR level using the 74-channel sensor configuration of the Magnes II Biomagnetometer (Biomagnetic Technologies, Inc.) Each epoch is 500 ms long and contains 260 samples in time. The signal is due to a 253 mm^2 patch of activity on the somatosensory cortex having a 2-D raised-cosine spatial extent. The signal time evolution is a Gaussian pulse of 22 ms full-width-at-half-maximum and peak amplitude at 148 ms relative to the onset. Noise from the prestimulus portion of evoked response data from a subject is added to the signal to obtain SNRs of 0, 5, 10, and 20 dB, where the SNR is defined as $\mathrm{tr}\left\{\mathbf{S}^T\mathbf{R}_s^{-1}\mathbf{S}\right\}$. Figure 1 depicts the average of 300 epochs for SNR = 10 dB after bandpass filtering between 1 Hz and 30 Hz. The beamspace transformation $\mathbf{F}$ is constructed to pass signals originating from a fairly large portion of cortex centered on the left hemisphere somatosensory region (identical to that in [10]). The beamspace dimension is 13, which is about a factor of six reduction from the original dimension of 74.

We construct four sets of cortical patches spanning the left hemisphere with average support of 70 mm^2 (3620 patches), 270 mm^2 (1208 patches), 590 mm^2 (586 patches), and 1000 mm^2 (341 patches). There is approximately fifty percent overlap between adjacent patches. The number of spatial basis functions associated with each patch is chosen as the number of singular values in (6) required to represent a given fractional signal level α. That is, we choose P as the smallest integer so that $\sum_{i=1}^{P}\sigma_i / \sum_{i=1}^{M}\sigma_i \geq \alpha$.

Patch localization is performed over five realizations of noise for each SNR level for various levels of α. This experiment reveals that choosing $\alpha = 0.8$ offers an excellent tradeoff between signal representation and patch differentiation. With $\alpha = 0.8$, the three largest patch sets correctly detect the patch containing the simulated activity in all cases, even with the lowest SNR (0 dB). Note that with the 70 mm^2 patch set the true activity is larger than any single patch. In this case the GLRT localized the activity to a patch within the extent of true activity.

Figure 2 illustrates the maximum likelihood estimate of the patch signal using $\alpha = 0.99$ to determine the number of bases in the patch and an SNR of 10 dB. The improvement over filtering and averaging (Fig. 1) is evident. Figure 3 depicts the reconstructed images of the peak patch signal amplitude (148 ms) for the 10 dB SNR data and the 590 mm^2 patch set. The true activity distribution is shown in Fig. 3(a). Figure 3(b) depicts the minimum norm solution to the local inverse problem based on the ML signal estimate shown in Fig. 2 whereas Fig. 3(c) depicts the solution using the filtered and averaged signal shown in Fig. 1. The activity estimated using ML is blurred relative to the true distribution, but has approximately correct amplitude, while the activity estimated from the filtered and averaged signal does not resemble the true activity and is four orders of magnitude larger.

We also collected 300 epochs of evoked response data using the same 74-channel configuration used to generate the simulated data by stimulating the right-hand index finger of a female subject with uniform pneumatic pressure pulses. Each epoch is 500 ms long with a 520.8 Hz sampling rate. Figure 4(a) depicts the result of patch localization using the 590 mm^2 patch set. The most significant patch is located near the lower portion of the somatosensory region, consistent with anatomical expectations. Figure 4(b) depicts the solution to the local inverse problem on the patch using the ML estimate of

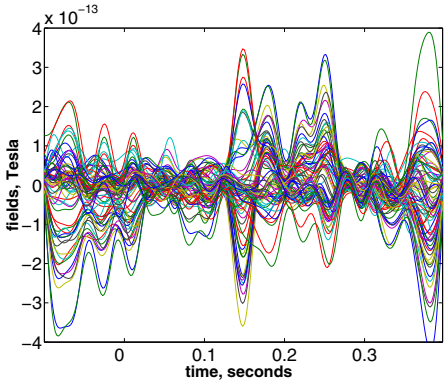

Fig. 1. Filtered (1-30 Hz) and averaged (300 epochs) synthetic signal plus real noise at SNR = 10 dB.

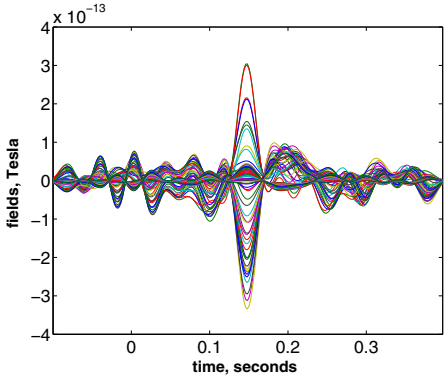

Fig. 2. ML estimate of the synthetic signal plus real noise at SNR = 10 dB after localizing the patch containing the signal.

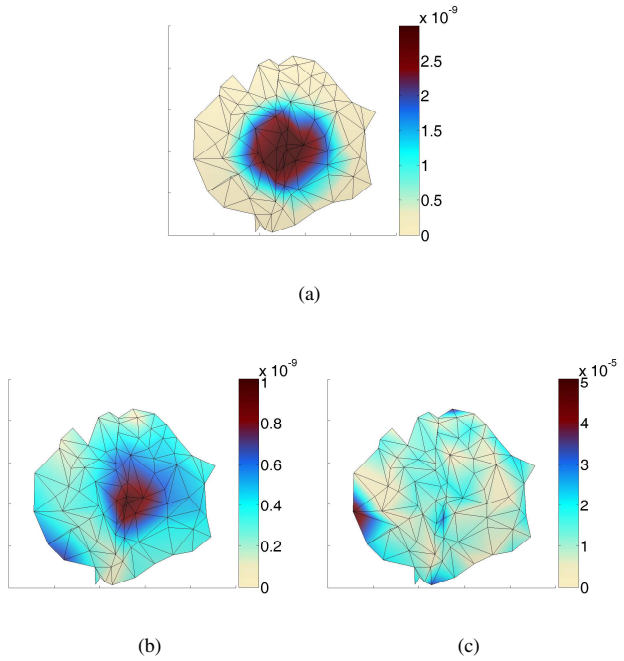

Fig. 3. Reconstructed images of patch activity for synthetic signal plus real noise at 10 dB SNR. Patch detection is performed using the 590 mm^2 patch set. (a) True activity distribution. (b) Reconstructed activity using ML signal estimate in Fig. 2. (c) Reconstructed activity using filter-and-average signal estimate in Fig. 1.

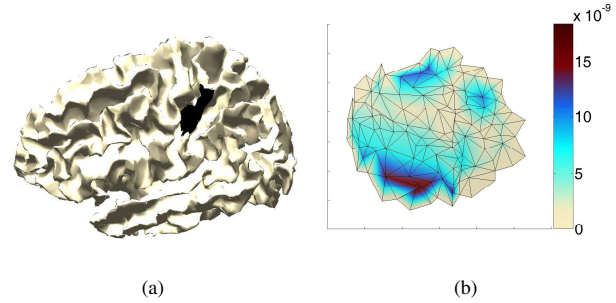

Fig. 4. Results for 300 epochs of index finger stimulation data. (a) Patch localization using the 590 mm^2 patch set. (b) Reconstructed activity on the patch.

the patch signal. The distribution of activity is relatively focal, as expected.

IV. Discussion

The GLRT and ML signal estimates assume an unknown spatial noise covariance matrix, and thus automatically incorporate noise whitening based on the measured data. The noise covariance matrix required for whitening the data is estimated from the portion of data containing the signal by exploiting the spatio-temporal structure of the evoked response paradigm and thus the assumption of stationarity between the pre- and post-stimulus intervals is not required, as noted in [6] and [7]. Implementing the GLRT and ML estimation in beamspace increases the robustness of the results, especially with low SNR or small numbers of epochs (see [10]).

Use of spatial bases for representing cortical patches provides a flexible approach to localization and signal estimation. It is desirable to use fewer bases for each patch in the localization stage to increase the differentiation between the spaces associated with each patch. The mismatch associated with not completely representing the signal in the correct patch is more than offset by the reduced leakage of the signal into other patches. However, once the patch is localized, the number of bases used to represent the patch is increased to facilitate accurate patch signal estimation.

Patch localization significantly reduces the difficulty of estimating the distribution of brain activity since the local inverse problem for the patch is much better conditioned than the global inverse problem.

References

[1] W. Kincses, C. Braun, S. Kaiser, and T. Elbert, "Modeling extended sources of event-related potentials using anatomical and physiological constraints," *Human Brain Mapping*, vol. 8, pp. 182–193, 1999.

[2] M. Wagner, Th. Köhler, M. Fuchs, and J. Kastner, "An extended source model for current density reconstructions," in *Proceedings of the 12th International Conference on Biomagnetism*, J. Nenonen, R. Ilmoniemi, and T. Katila, Eds. Espoo, Finland: Espoo: Helsinki Univ. of Technology, Aug 2000, pp. 749–752.

[3] K. Jerbi, J. Mosher, G. Nolte, S. Baillet, L. Garnero, and R. Leahy, "From dipoles to multipoles: Parametric solutions to the inverse problem in MEG," in *Proceedings of the 13th International Conference on Biomagnetism*, Jena, Germany, Aug 2002.

[4] G. Nolte and G. Curio, "Current multipole expansion to estimate lateral extent of neuronal activity: A theoretical analysis," *IEEE Trans Biomed. Eng.*, vol. 47, no. 10, pp. 1347–1355, 2000.

[5] J. Mosher, R. Leahy, D. Shattuck, and S. Baillet, "MEG source imaging using multipolar expansions," in *Lecture Notes in Computer Science*, vol. 1613, Proc. IPMI99. Springer-Verlag GmbH, 1999.

[6] A. Dogandžić and A. Nehorai, "Estimating evoked dipole responses in unknown spatially correlated noise with EEG/MEG arrays," *IEEE Trans Signal Processing*, vol. 48, no. 1, pp. 13–25, 2000.

[7] B. Baryshnikov, B. Van Veen, and R. Wakai, "Maximum-likelihood estimation of low-rank signals for multiepoch MEG/EEG analysis," *IEEE Trans Biomed. Eng.*, vol. 51, no. 11, pp. 1981–1993, 2004.

[8] R. Srebro, "An iterative approach to the solution of the inverse problem," *Electroencephalography and clinical Neurophysiology*, vol. 98, pp. 349–362, 1996.

[9] L. Gavit, S. Baillet, J. Mangin, J. Pescatore, and L. Garnero, "A multiresolution framework to MEG/EEG source imaging," *IEEE Trans Biomed. Eng.*, vol. 48, no. 10, pp. 1080–1087, 2001.

[10] A. Rodríguez-Rivera, B. Baryshnikov, B. Van Veen, and R. Wakai, "MEG and EEG source localization in beamspace," *IEEE Trans Biomed. Eng.*, in review.

[11] A. Rodríguez-Rivera, B. Van Veen, and R. Wakai, "Bootstrap investigation of linearly constrained minimum variance localization in subspaces," in *Proceedings of the 14th International Conference on Biomagnetism*, E. Halgren, S. Ahlfors, M. Hämäläinen, and D. Cohen, Eds. Boston, MA: Biomag 2004 Ltd., Aug 2004, pp. 585–586.

[12] R. Muirhead, *Aspects of multivariate statistical theory*. New York: John Wiley & Sons, Inc., 1982.

[13] M. Zoltowski and T. Lee, "Maximum likelihood based sensor array signal processing in the beamspace domain for low angle radar tracking," *IEEE Trans Signal Processing*, vol. 39, pp. 656–671, 1991.

[14] H. Lee and M. Wengrovitz, "Resolution threshold of beamspace MUSIC for two closely spaced emitters," *IEEE Trans Signal Processing*, vol. 38, no. 9, pp. 1545–1559, 1990.

[15] E. Kelly and K. Forsythe, "Adaptive detection and parameter estimation for multidimensional signal models," Lincoln Laboratory, Lexington, MA, Tech. Rep. 848, April 1989.